A Model Predictive Controller with Adaptive Tuning Weights for Energy Management in Fuel Cell Hybrid Electric Vehicles

Qian Xun
RISE Research Institutes of Sweden
Bors 50462, Sweden
Email: qian.xun@ri.se

Qiuyu Li and Hengzhao Yang*
ShanghaiTech University
Shanghai 201210, China
Email: {liqy1, hzyang}@shanghaitech.edu.cn

***Abstract*—Fuel cell hybrid electric vehicles (FCHEVs) are recognized as a promising solution for vehicle electrification. However, the adoption of FCHEVs is relatively slow due to various factors such as the high cost of hydrogen and the limited lifespan of fuel cells. Therefore, effective energy management strategies are of great interest. Model predictive control (MPC) is widely employed to deal with energy management in FCHEVs. However, conventional MPC often relies on subjective selection of control weights in the objective function and the performance may be compromised. This paper proposes an optimal weight adaptation method within the MPC framework to enhance its effectiveness. The weights in the objective function are dynamically adjusted online using a moving horizon. Optimization techniques are then applied to fine tune these weights. The effectiveness of the proposed MPC controller with adaptive tuning weights is validated under the UDDS drive cycle.**

***Index Terms*—Fuel cell hybrid electric vehicles, model predictive control, optimal weight adaptation, energy management.**

I. Introduction

Fuel cell hybrid electric vehicles (FCHEVs) represent a promising avenue for mitigating the environmental concerns associated with traditional internal combustion engine (ICE) technology [1]. Despite their potential, FCHEVs still face performance challenges that require attention. For instance, the longevity of fuel cells (FCs) has yet to meet the targets set by the U.S. Department of Energy (DoE), while the cost of hydrogen remains relatively high [2]. As such, there is a pressing need for the development of sophisticated energy management strategies aimed at not only prolonging FC lifetimes but also minimizing hydrogen consumption [3]–[5].

The energy management strategies are typically categorized into rule-based and optimization-based approaches [6]–[8], while the latter includes off-line optimized control and online real-time control. Off-line optimization methods are commonly utilized to assess the performance of online controllers. In such applications, foreknowledge of driving patterns and routes is assumed. However, online controllers become imperative when future driving conditions are uncertain. Presently, online power management strategies rely on rules and optimization techniques. While rule-based strategies are conceptually straightforward, their performance often falls short of optimal. Moreover, incorporating various rules becomes challenging, particularly in real-time implementation, especially as system complexity escalates.

Model predictive control (MPC) is widely embraced as an effective approach for addressing multi-objective problems [9], [10]. Also referred to as receding horizon control, MPC involves predicting the optimal control input within a finite time horizon based on current sampled states. In [11], [12], MPC is formulated for FCHEVs to allocate power between the FC and the battery, aiming to minimize hydrogen consumption, FC degradation, and battery state of charge (SoC) variation. However, determining the control weights of the corresponding states and control inputs in their objective functions relies on human-expert knowledge. Moreover, using fixed weights in the objective functions results in power allocation with a fixed ratio between the FC and the battery. Therefore, this approach may not always yield optimal operational results.

To address this challenge, recent literature proposes adaptive MPC methods [13], [14]. In [15], a linear parameter-varying (LPV) prediction model is introduced for an MPC controller in FCHEVs. This model dynamically updates online based on variations in battery SoC. Similarly, [16] presents an adaptive Pontryagin's Minimum Principle (PMP) based MPC for an FC hybrid railway vehicle. Here, an online adaptive estimated co-state is integrated into PMP to optimize power distribution and battery SoC. Additionally, MPC with adaptive tuning weights offers a method for adaptive power allocation. In [17], an adaptive weight determined by fuzzy logic rules is proposed for the MPC energy management strategy, allocating power between the battery and supercapacitor in a hybrid energy storage system for vehicles. Inspired by these approaches, this paper introduces adaptive tuning weights within the MPC framework to enhance hydrogen economy, prolong FC lifetime, and mitigate SoC fluctuations.

The remainder of this paper is organized as follows. Section II presents the FCHEV system architecture and component models. Section III designs the MPC controller with adaptive tuning weights. Section IV shows the simulation results. Section V concludes this paper.

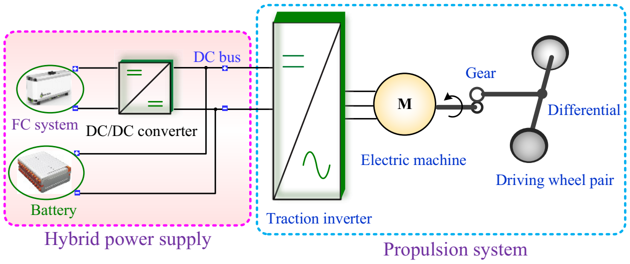

Fig. 1. System architecture of FCHEV.

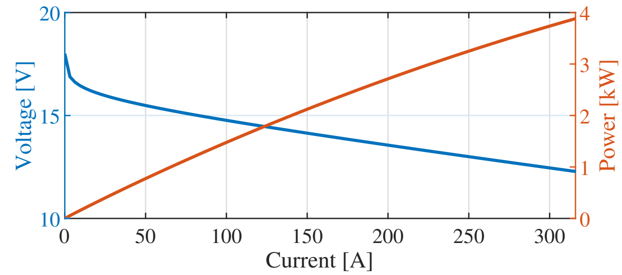

Fig. 2. Polarization curve of fuel cell stack.

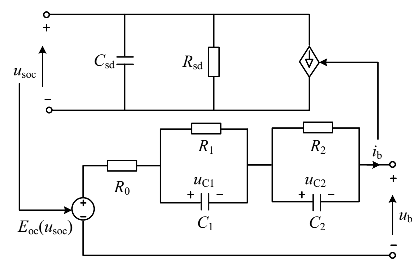

Fig. 3. Equivalent circuit model of battery.

II. System Architecture and Component Models

The FCHEV powertrain structure investigated in this paper is depicted in Fig. 1, encompassing both a hybrid power supply and a propulsion system. The hybrid power supply comprises an FC, a battery, and a DC/DC converter. The DC/DC converter serves to elevate the FC voltage for seamless integration with the battery, enhancing overall efficiency and dynamics. In addition, the propulsion system consists of a traction inverter, electric machine, gear assembly, differential, and driving wheel pair. Each component plays a crucial role in facilitating the conversion of energy and the transmission of power to propel the vehicle.

A. Plant Model

1) Fuel Cell Model: An FC is an energy conversion device that converts hydrogen energy into electrical energy. Its output voltage typically diminishes as the operating current increases, a characteristic depicted by the polarization curve. In this study, a 3.9 kW FC stack as referenced in [18], is utilized. The polarization curve and its power curve, derived from a generalized model accessible in MATLAB/Simulink, are illustrated in Fig. 2. It is evident that the voltage exhibits an almost linear relationship with the current once the current surpasses a certain threshold. This relationship can be expressed as:

$$u_{\mathrm{fc}}(t) = f(i_{\mathrm{fc}}(t)), \tag{1}$$

where $u_{\mathrm{fc}}(t)$ represents the voltage of the FC stack and $i_{\mathrm{fc}}(t)$ denotes the current. The FC utilizes hydrogen energy to generate electric energy, with the mass flow rate of consumed hydrogen calculated as:

$$\dot{m}_{\mathrm{H2}}(t) = \frac{i_{\mathrm{fc}}(t) N_{\mathrm{fc}} M_{\mathrm{H2}}}{nF}. \tag{2}$$

Here, N_{fc} represents the number of cells in the stack, M_{H2} signifies the molar mass of hydrogen, n denotes the number of moles of electrons per mole of hydrogen, and F represents the Faraday constant. The hydrogen mass flow rate is denoted as $f_{\mathrm{H2}}(i_{\mathrm{fc}})(t)$.

2) Battery Model: In our case study, a lithium-ion battery is employed, and its voltage can be modeled as a controlled voltage source in series with a resistor and two RC branches, as depicted in Fig. 3. Parameters such as R_0, R_1, C_1, R_2, and C_2 represent the dynamic characteristics of the battery. Additionally, the controlled current source, coupled with R_{sd} and C_{sd}, represents the remaining capacity of the battery. The continuous state-space model of the battery can be derived according to Kirchhoff's law, which is described as:

$$\begin{cases} \dot{u}_1(t) = -\dfrac{1}{C_1 R_1} u_1(t) + \dfrac{1}{C_1} i_{\mathrm{b}}(t), \\ \dot{u}_2(t) = -\dfrac{1}{C_2 R_2} u_2(t) + \dfrac{1}{C_2} i_{\mathrm{b}}(t), \\ \dot{u}_{\mathrm{soc}}(t) = -\dfrac{1}{C_{\mathrm{sd}} R_{\mathrm{sd}}} u_{\mathrm{soc}}(t) - \dfrac{1}{C_{\mathrm{sd}}} i_b(t), \\ u_b(t) = E_{\mathrm{oc}}(u_{\mathrm{soc}}) - R_0 i_b(t) - u_1(t) - u_2(t). \end{cases} \tag{3}$$

In this context, $u_1(t)$ and $u_2(t)$ symbolize the voltages across the capacitors C_1 and C_2, while $u_{\mathrm{soc}}(t)$ represents the equivalent voltage corresponding to the SoC. The value of $u_{\mathrm{soc}}(t)$ is constrained between 0 and 1, indicating the SoC ranging from 0 to 100%. $u_{\mathrm{b}}(t)$ denotes the battery terminal voltage, and $i_{\mathrm{b}}(t)$ refers to the battery current. Furthermore, $E_{\mathrm{oc}}(u_{\mathrm{soc}})$ stands for the open-circuit voltage (OCV), expressed as a function of the battery SoC. Typically, the OCV is measured as a static variable and the OCV data of a battery cell is retrieved from [18] and then scaled to represent a module. Therefore, the OCV of the scaled battery module is graphically depicted in Fig. 4. The OCV ranges from 38.5 V to 48.5 V with an SoC from 0 to 100%. Furthermore, the OCV exhibits nearly linear behavior when the SoC varies from 20% to 80%.

3) Vehicle Model: For simplification, the vehicle propulsion system is modeled as a current load controlled by the current demand of the vehicle system. Within this framework, the current load is computed from the total power demand, which is the summation of the wheel power demand and the auxiliary

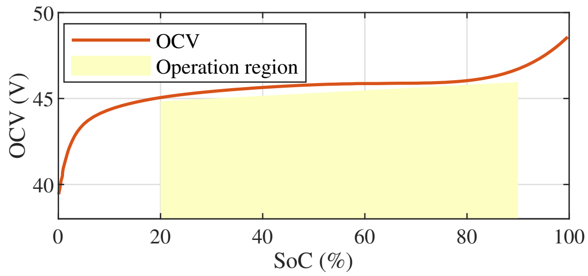

Fig. 4. Relationship between OCV and SoC.

power. The wheel power is described by:

$$\begin{aligned} F_{\text{wheel}}(t) =& 0.5\rho_{\text{air}}C_{\text{d}}v^2(t) + ma(t) + \\ & mg\left(\sin\alpha(t) + C_{\text{r}}\cos\alpha(t)\right), \\ P_{\text{wheel}}(t) =& F_{\text{wheel}}(t)v(t) + P_{\text{aux}}, \end{aligned} \quad (4)$$

where ρ_{air}, C_{d}, C_{r}, m, and g represent the air density, air resistance coefficient, rolling resistance coefficient, vehicle mass, and gravitational constant, respectively. $v(t)$ and $a(t)$ are the vehicle speed and acceleration, respectively, while $\alpha(t)$ denotes the road slope. Additionally, the auxiliary power is denoted as P_{aux}.

4) DC/DC Converter Model: A boost converter serves as the DC/DC converter to bridge the voltage gap between the FC and the battery. The current change rate of the boost converter can be expressed as

$$\dot{i}_{\text{boost}}(t) = \Delta i_{\text{boost}}(t), \quad (5)$$

where $i_{\text{boost}}(t)$ represents the current through the boost converter at the battery side, and $\Delta i_{\text{boost}}(t)$ denotes the change rate of $i_{\text{boost}}(t)$. At steady state, the following equation holds:

$$\eta_{\text{boost}}u_{\text{fc}}(t)i_{\text{fc}}(t) = u_{\text{b}}(t)i_{\text{boost}}(t), \quad (6)$$

where η_{boost} represents the efficiency of the boost converter. As the boost converter, battery, and the load are connected in parallel, the current balance in the DC-link is governed by

$$i_{\text{boot}}(t) + i_{\text{b}}(t) = i_{\text{load}}(t), \quad (7)$$

where $i_{\text{load}}(t)$ denotes the current demand of the vehicle, which can be calculated as $i_{\text{load}} = \frac{P_{\text{wheel}}(t)}{k_{\text{v}}u_{\text{b}}(t)}$ with k_{v} being a scaling factor.

B. Controller Model

The controller operates in a discrete domain. By employing Euler discretization with a sampling period of T, we can obtain the discrete state-space model. In the discrete domain, the dynamics of the battery voltage and the SoC can be derived from (3), as follows

$$\begin{cases} u_1(k+1) = \left(1 - \dfrac{T}{C_1R_1}\right)u_1(k) + \dfrac{T}{C_1}i_{\text{b}}(k), \\ u_2(k+1) = \left(1 - \dfrac{T}{C_2R_2}\right)u_2(k) + \dfrac{2}{C_2}i_{\text{b}}(k), \\ u_{\text{soc}}(k+1) = \left(1 - \dfrac{T}{C_{\text{sd}}R_{\text{sd}}}\right)u_{\text{soc}}(k) - \dfrac{T}{C_{\text{sd}}}i_{\text{b}}(k) \end{cases} \quad (8)$$

Consequently, these three states are bounded as

$$\begin{cases} u_{1,\min} \leqslant u_1(k) \leqslant u_{1,\max}, \\ u_{2,\min} \leqslant u_2(k) \leqslant u_{2,\max}, \\ u_{\text{soc},\min} \leqslant u_{\text{soc}}(k) \leqslant u_{\text{soc},\max}. \end{cases} \quad (9)$$

Similarly, the discrete state-space model of the boost converter can be derived as

$$i_{\text{boost}}(k+1) = i_{\text{boost}}(k) + T\Delta i_{\text{boost}}(k), \quad (10)$$

where $\Delta i_{\text{boost}}(k)$ is bounded

$$\Delta i_{\text{boost},\min} \leqslant \Delta i_{\text{boost}}(k) \leqslant \Delta i_{\text{boost},\max}. \quad (11)$$

III. Energy Management Framework

A. Prediction Model

The objective of energy management is to regulate the power distribution between the FC and the battery to enhance hydrogen economy and FC lifetime, while minimizing SoC fluctuations. Ignoring power loss of the DC/DC converter, the output power equals the input power referring to the FC power. Hence, controlling the FC power is reflected by controlling the output power of the DC/DC converter. Since the battery is directly connected to the output of the boost converter, they share the same output voltage. Furthermore, the current balance is governed by (7), requiring only one decision variable, either $i_{\text{boost}}(t)$ or $i_{\text{b}}(t)$, with the other indirectly controlled. In our study, $i_{\text{boost}}(t)$ is chosen as the decision variable for energy management. To calculate $i_{\text{boost}}(t)$, the current change rate can be obtained by the MPC controller. Consequently, the current change rate of the boost converter is selected as the system input, while the output current of the boost converter and the voltage across capacitor C_{sd} are chosen as the state variables. The state-space equation is written in a compact form as

$$x^+ = Ax + B_{\text{u}}u + B_{\text{d}}d, \quad (12)$$

where x^+ is the value of the state x at the next sample, x is the state vector at the current sample and u is the control input vector, which can be described as $x = [i_{\text{boost}}, u_{\text{soc}}]^{\text{T}}$, $u = \Delta i_{\text{boost}}$,$d = i_{\text{load}}$.

B. Problem Formulation

To minimize hydrogen consumption, FC degradation, and battery SoC fluctuations, the performance indicators are defined:

(1) The battery SoC should be regulated between maximum and minimum values while fluctuating around the reference $u_{\text{soc,ref}}$. Thus, the first objective is to minimize $\|u_{\text{soc}} - u_{\text{soc,ref}}\|$;

(2) As indicated in (2), the mass flow rate of hydrogen in an FC stack is proportional to its current. Therefore, to reduce hydrogen consumption $f_{\text{H2}}(i_{\text{fc}})(t)$, FC current $\|i_{\text{fc}}\|$ should be minimized, which translates to minimizing the DC/DC converter current $\|i_{\text{boost}}\|$;

(3) FC degradation is influenced by the current change rate, and minimizing $\|\Delta i_{\text{fc}}\|$ is necessary. Similarly, minimization

of $\|\Delta i_{\mathrm{fc}}\|$ is expressed as minimizing $\|\Delta i_{\mathrm{boost}}\|$ since i_{boost} is directly related to i_{fc}.

In summary, with weight coefficients ω_1, ω_2, and ω_3 introduced, the cost function to be optimized is formulated as

$$\begin{aligned}&\min_{u_0,u_1,\dots}\sum_{k=0}^{\infty}h(x_k,u_k)\\&=\min_{u_0,u_1,\dots}\sum_{k=0}^{\infty}\begin{pmatrix}\omega_1\left\|u_{\mathrm{soc,k}}-u_{\mathrm{soc,ref}}\right\|^2\\+\omega_2\left\|i_{\mathrm{boost,k}}\right\|^2+\omega_3\left\|\Delta i_{\mathrm{boost,k}}\right\|^2\end{pmatrix}.\end{aligned}\tag{13}$$

The problem described in (13) is commonly addressed by solving the optimization problem over a finite time horizon N considering relevant constraints and system dynamics, while continuously measuring the system state to recompute new control sequences with updated information. This iterative procedure can be expressed as

$$\begin{aligned}&\min_{u_0,u_1,\dots}\sum_{k=0}^{N-1}\left((x_k-x_{\mathrm{ref}})^{\mathrm{T}}Q(x_k-x_{\mathrm{ref}})+u_k^{\mathrm{T}}Ru_k\right)\\&\quad+x(N)^{\mathrm{T}}P_f x(N),\\&\text{s.t.}\, x_{k+1}=Ax_k+B_{\mathrm{u}}u_k+B_{\mathrm{d}}d,\\&\quad x(0)=x_0,\\&\quad G(x,u)=0,\\&\quad H(x,u)\leqslant 0,\end{aligned}\tag{14}$$

where Q and R are penalty matrices for the state and control sequences, and $x_{\mathrm{ref}}=\begin{bmatrix}u_{\mathrm{SoC_{ref}}} & 0\end{bmatrix}^{\mathrm{T}}$. x_0 represents the system state at the current time sample, $G(x,u)$ comprises all equality constraints, and $H(x,u)$ represents all inequality constraints. At each time sample k, the optimal sequence of states and control inputs over a finite time horizon N is defined as:

$$\begin{cases}\mathbf{x}^*\triangleq\left\{x(0),x(1),\cdots,x(N)\right\},\\\mathbf{u}^*\triangleq\left\{u(0),u(1),\cdots,u(N-1)\right\}.\end{cases}\tag{15}$$

C. Adaptive Tuning Weights

The true cost associated with using MPC with a set of weights $\omega=\omega_1,\omega_2,\omega_3$ is defined as $J_{\mathrm{true}}^{\omega}(x_k,u_k)$. Following simulations or experiments and evaluating the state and control trajectories of the plant, the true cost function J_{true} can be obtained. The objective of adaptive weight tuning is to determine the optimal weights for the individual objective functions that minimize the expected true cost, given a prior distribution of initial conditions $x(0)$. Therefore, the optimization problem can be formulated as

$$\omega^*=\arg\min\overline{J}_{\mathrm{true}}^{\omega}(x_k,u_k),\tag{16}$$

where ω^* represents the set of optimal weights, and the expected true cost can be approximately calculated by the average true cost:

$$\overline{J}_{\mathrm{true}}^{\omega}(x_k,u_k)=\mathop{\mathbb{E}}_{x(0)}[J_{\mathrm{true}}^{\omega}(x_k,u_k)].\tag{17}$$

Solving the problem formulated in (16) is computationally expensive, and the expected true cost is a black-box to the optimization variable ω^*. Consequently, the true cost is approximated to evaluate the objective function by providing a control input through solving (14) without constraints.

D. Implementation of MPC with Adaptive Tuning Weights

The entire procedure of MPC with the adaptive tuning weights is summarized in Algorithm 1.

Algorithm 1: MPC with Adaptive Tuning Weights

Input: x_0, N
Output: $u(0)$
Set $k=0$ for the time sample in a drive cycle;
while *not at the end of the drive cycle* **do**
  Update the system state x_0;
  Set the initial state $x(k)=x_0$;
  Obtain an optimal control sequence $\mathbf{u}$ by solving problem (14) without constraints;
  for $j=1$*;* $j\leq N$*;* $j++$*;* **do**
    Compute true cost at the j^{th} iteration $J_{\mathrm{true}}^{\omega,j}(x_k^j,u_k^j)$;
  end
  Solve the problem $\min\overline{J}_{\mathrm{true}}^{\omega}(x_k^j,u_k^j)$;
  Obtain the optimal weight ω^*;
  Apply the optimal weight ω^* to the problem (14) and obtain the optimal control sequences $\mathbf{u}^*$;
  Apply the first element of the control sequences $u(0)$ as the control input at next time sample;
  Return $u(0)$;
  Let $k:=k+1$
end

IV. Simulation Results

To verify the effectiveness of the formulated MPC with the adaptive tuning weights, simulations are performed in MATLAB 2023b on a PC equipped with a 4.2 GHz Intel Core i-7700K and 64 GB RAM. The EPA Urban Dynamometer Driving Schedule (UDDS) drive cycle is selected for the study case. Vehicle parameters are referenced from [3] with a scaling factor to scale down the power demand.

Fig. 5 depicts the simulation results for power allocation, current allocation, FC current change rate, and battery SoC under the UDDS drive cycle test. The controller endeavors to minimize FC hydrogen consumption and battery SoC fluctuation, effectively managing power distribution. The FC operation power fluctuates around the load power with a small change rate, as the FC current change rate remains within 20 A/s. Particularly during the extra high-speed region and high power demand phases of the drive cycle, the FC current change rate hovers around 19 A/s. This allows the battery to handle the high-frequency component in the power demand while the FC primarily provides a smaller frequency portion. Additionally, the battery SoC fluctuates around its reference value, set at 60% in the simulation.

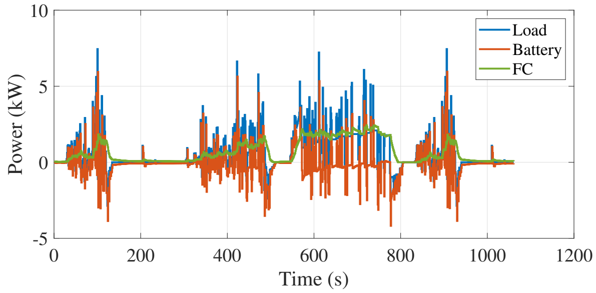

(a) Power allocation.

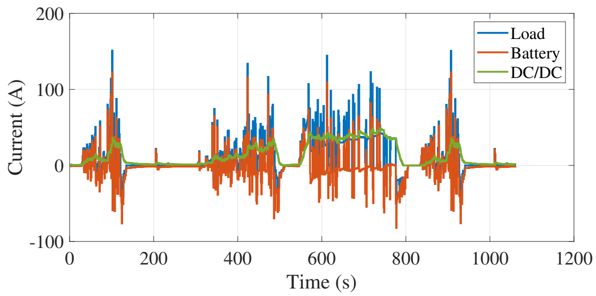

(b) Current allocation.

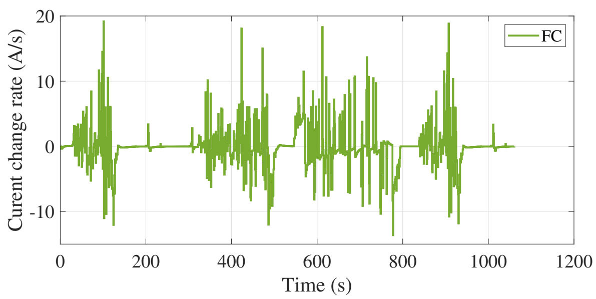

(c) FC current change rate.

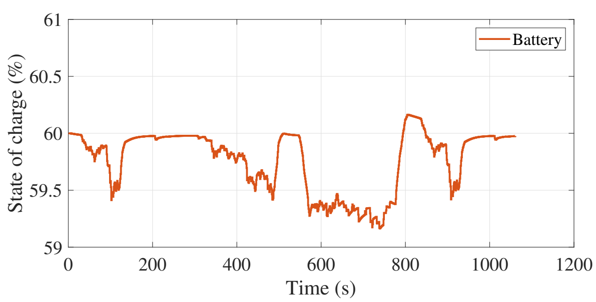

(d) Battery SoC.

Fig. 5. Simulation results under UDDS drive cycle.

V. Conclusion

This paper proposes an energy management strategy based on an MPC controller with adaptive tuning weights to address three aspects of FCHEVs: hydrogen consumption, FC degradation, and battery SoC fluctuation. The weights are dynamically tuned using a moving horizon. The effectiveness of the proposed MPC controller is validated through MATLAB simulations under the UDDS drive cycle. Simulation results show that the FC current change rate and the battery SoC are effectively controlled within specified ranges while the hydrogen consumption is minimized whenever feasible.

References

[1] Q. Xun, S. Lundberg, and Y. Liu, "Design and experimental verification of a fuel cell/supercapacitor passive configuration for a light vehicle," *Journal of Energy Storage*, vol. 33, p. 102110, 2021.

[2] D. Papageorgopoulos, "Fuel cell R&D overview," in *Annual Merit Review and Peer Evaluation Meeting*, 2019.

[3] Q. Xun, N. Murgovski, and Y. Liu, "Joint component sizing and energy management for fuel cell hybrid electric trucks," *IEEE Transactions on Vehicular Technology*, vol. 71, no. 5, pp. 4863–4878, 2022.

[4] M. Kandidayeni, A. Macias, L. Boulon, and S. Kelouwani, "Efficiency upgrade of hybrid fuel cell vehicles energy management strategies by online systemic management of fuel cell," *IEEE Transactions on Industrial Electronics*, vol. 68, no. 6, pp. 4941–4953, 2021.

[5] Q. Xun, N. Murgovski, and Y. Liu, "Chance-constrained robust co-design optimization for fuel cell hybrid electric trucks," *Applied Energy*, vol. 320, p. 119252, 2022.

[6] J. Wu, Y. Zhang, J. Ruan, Z. Liang, and K. Liu, "Rule and optimization combined real-time energy management strategy for minimizing cost of fuel cell hybrid electric vehicles," *Energy*, vol. 285, p. 129442, 2023.

[7] H.-B. Yuan, W.-J. Zou, S. Jung, and Y.-B. Kim, "A real-time rule-based energy management strategy with multi-objective optimization for a fuel cell hybrid electric vehicle," *IEEE Access*, vol. 10, pp. 102 618–102 628, 2022.

[8] Q. Xun, V. Roda, Y. Liu, X. Huang, and R. Costa-Castelló, "An adaptive power split strategy with a load disturbance compensator for fuel cell/supercapacitor powertrains," *Journal of Energy Storage*, vol. 44, p. 103341, 2021.

[9] H. He, S. Quan, F. Sun, and et al, "Model predictive control with lifetime constraints based energy management strategy for proton exchange membrane fuel cell hybrid power systems," *IEEE Transactions on Industrial Electronics*, vol. 67, no. 10, pp. 9012–9023, 2020.

[10] Q. Li and H. Yang, "Evaluation of two model predictive control schemes with different error compensation strategies for power management in fuel cell hybrid electric buses," *Journal of Energy Storage*, vol. 72, p. 108148, 2023.

[11] H. Chen, J. Chen, H. Lu, and et al, "A modified MPC-based optimal strategy of power management for fuel cell hybrid vehicles," *IEEE/ASME Transactions on Mechatronics*, vol. 25, no. 4, pp. 2009–2018, 2021.

[12] D. F. Pereira, F. C. Lopes, and E. H. Vantanabe, "Nonlinear model predictive control for the energy management of fuel cell hybrid electric vehicles in real-time," *IEEE Transactions on Industrial Electronics*, vol. 68, no. 4, pp. 3213–3223, 2021.

[13] D. Kostadinov and D. Scaramuzza, "Online weight-adaptive nonlinear model predictive control," in *2020 IEEE/RSJ International Conference on Intelligent Robots and Systems (IROS)*, 2020, pp. 1180–1185.

[14] V.-A. Le and A. A. Malikopoulos, "Optimal weight adaptation of model predictive control for connected and automated vehicles in mixed traffic with Bayesian optimization," in *2023 American Control Conference (ACC)*, 2023, pp. 1183–1188.

[15] C. Jia, W. Qiao, J. Cui, and L. Qu, "Adaptive model-predictive-control-based real-time energy management of fuel cell hybrid electric vehicles," *IEEE Transactions on Power Electronics*, vol. 38, no. 2, pp. 2681–2694, 2023.

[16] K. Deng, H. Peng, S. Dirkes, J. Gottschalk, C. Ünlübayir, A. Thul, L. Löwenstein, S. Pischinger, and K. Hameyer, "An adaptive PMP-based model predictive energy management strategy for fuel cell hybrid railway vehicles," *eTransportation*, vol. 7, p. 100094, 2021.

[17] B. Ma, X. Guo, and P. Li, "Adaptive energy management strategy based on a model predictive control with real-time tuning weight for hybrid energy storage system," *Energy*, vol. 283, p. 129128, 2023.

[18] H. Chen, J. Chen, C. Wu, and H. Liu, "Fuzzy logic based energy management for fuel cell/battery hybrid systems," in *2018 European Control Conference (ECC)*, 2018, pp. 89–94.